SPECIAL PROJECT PROGRESS REPORT

All the following mandatory information needs to be provided. The length should *reflect the complexity and duration* of the project.

Reporting year	2022…………………………………..……
Project Title:	Diabatic heating rates and moist tendencies along airstreams associated with different weather systems
Computer Project Account:	SPCHBOJO……………………………………..……
Principal Investigator(s):	Hanin Binder, Hanna Joos…………..……
Affiliation:	ETH Zürich, Institute for Atmospheric and Climate Science, Zurich, Switzerland
Name of ECMWF scientist(s) collaborating to the project (if applicable)	Dr. Richard Forbes
Start date of the project:	1. January 2021…………………………..……
Expected end date:	31. December 2023………………………..……

Computer resources allocated/used for the current year and the previous one
(if applicable)
Please answer for all project resources

		Previous year		Current year	
		Allocated	Used	Allocated	Used
High Performance Computing Facility	(units)	1 000 000	320 000	800 000	0
Data storage capacity	(Gbytes)	20 000		43 000	0

Summary of project objectives (10 lines max)

In this project we make use of our special IFS version that allows to output hourly all moisture, temperature and momentum tendencies from the parameterized physics. We will use these tendencies in order to increase our knowledge about the hydrological cycle in different regions of the world as well as to improve our understanding of their interaction with the atmospheric circulation by modifying the potential vorticity in the tropopause region, in warm conveyor belts and in Mediterranean cyclones and we investigate the importance of radiative tendencies for extratropical dynamics.

Summary of problems encountered (10 lines max)

No problems encountered.

Summary of plans for the continuation of the project (10 lines max)

A dedicated IFS simulation was performed, initialized at 00 UTC 26 February 2019. The aim is to study: (i) an event of clear air turbulence (CAT) over Iran; and (ii) to investiagte how this CAT event relates to negative values of potential vorticity (PV) at the CAT location. To this aim, the extra fields of the dedicated IFS simulation will be used to analyse the origin and mechanisms leading to the CAT and negative PV. In another project we are analyzing the effect of radiative heating rates on extratropical dynamics based on the 1-year IFS simulation with the detailed hourly output which has been performed during the last special project. Furthermore we will use this 1-year simulation in order to investigate the impact of below-cloud cooling processes on the dynamics in extratropical cyclones. In a collaboration with KIT, Germany we will continue the detailed comparison of diabatic heating and PV rates in the IFS and an ICON simulation.

List of publications/reports from the project with complete references

Mueller, S., Diabatic processes associated with an extratropical dry intrusion reaching into the western North Atlantic trade wind region, MSc thesis ETH Zuerich, 2021, supervised by F. Aemisegger, M. Boettcher and L. Villiger

Eschle, S., Moisture cycle in an extratropical cyclone, MSc thesis ETH Zuerich, 2022, supervised by M. Böttcher, H.Binder and H. Joos

Müller, S., Boettcher, M., Villiger, L. and Aemisegger. F., The impact of diabatic processes on an extratropical dry intrusion entering into the boundary layer in the western North Atlantic trade wind region, in prep. for ACPD

Summary of results

1) Heat and moisture budget of an extratropical dry intrusion into the North Atlantic trades (Dr. Franziska Aemisegger, Leonie Villiger, Dr. Maxi Boettcher)

Intrusions of dry upper-level extratropical air into the tropics play an important role in shaping the synoptic time-scale variability of the low-level cloud cover over the subtropical and tropical oceans (Aemisegger et al. 2021). An Integrated Forecasting System (IFS) simulation with heating rate and moist tendency output (0.4° horizontal resolution, 137 vertical levels) has been performed for an extratropical dry intrusion (EDI) reaching the Caribbean at the end of January 2018 (Fig. 1a). The case has been studied extensively in a Master Thesis (Mueller, 2021). The three aims of this research are to
(1) analyse the heat and humidity budget along a North Atlantic EDI during its descent,
(2) quantify the impact of boundary layer clouds on the EDI's heat and moisture budget, and

(3) study the interaction of the EDI with the cold front and its impact on the cold front's southward propagation.

In this WP, we have performed a detailed Lagrangian analysis of the EDI in the IFS simulation for the end of January 2018. During this period, the easterly trade winds were interrupted for several days by a coherent airstream consisting of rapidly descending air parcels reaching from the mid-latitude jet stream region into the sub-cloud layer in the trades (Fig 1a). As those air parcels were anomalously dry and cold, they had a notable impact on diabatic processes in the vicinity of the trade-wind cloud tops such as primarily longwave cooling but also cloud evaporation and sublimation (Fig 2). To quantify the Lagrangian heat and moisture budget along the EDI, we analyzed the individual diabatic heating rates (DHR) and moist tendencies (QVR) along Lagrangian trajectories based on hourly three-dimensional wind fields.
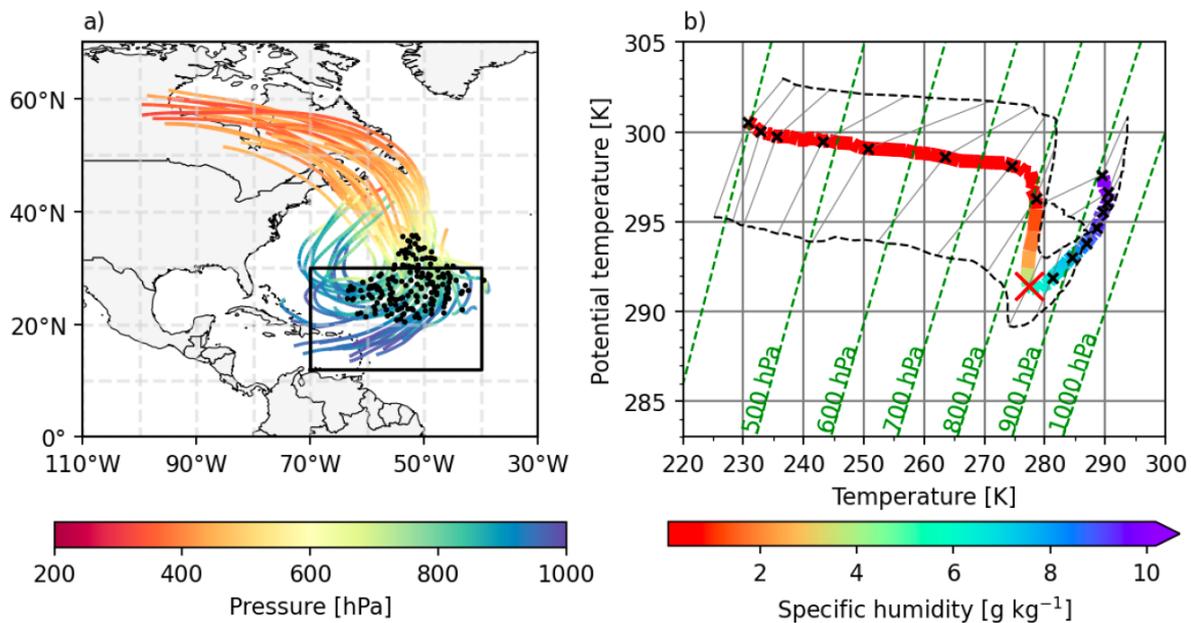

Fig. 1: Temporal evolution of thermodynamic conditions associated with EDI trajectories shown for the interval [tBLH -48 h, tBLH +48 h] with tBLH the time of entry of the air parcels into the boundary layer. (a) Descent and outflow of the DI with trajectories colored with pressure and tBLH indicated for every trajectory by a black dot. (b) Temporal evolution of the median temperature T and potential temperature (q) with the median specific humidity of the EDI trajectories in colors in the $T–q$ phase space synchronised with respect to tBLH (red cross). The black crosses indicate 6 hourly time steps relative to tBLH and the black dashed lines the 25th and 75th percentiles of the $T– q$ conditions along the EDI trajectories. The green dashed lines represent isobars.

In the first part of their descent from the mid-tropospheric jet stream region, the EDI air parcels' heat budget is dominated by adiabatic warming of about 1 K h^{-1} and they conserve their initial upper tropospheric humidity (Fig. 1b and 2). In the second part of their descent, they experience strong diabatic cooling of about -0.8 K h^{-1} and moistening at cloud tops of about 0.8 g kg h^{-1} (Fig. 1b and 2b).

The diabatic cooling is mainly due to radiative (-0.5 K h^{-1}) and microphysical processes (-0.3 K h^{-1}) and to a lesser extent due to turbulent cooling (-0.05 K h^{-1}). This diabatic cooling at cloud tops leads to cross-isentropic flow, which allows the EDI air parcels to pass through the inversion and to penetrate into the boundary layer. Thereafter, the EDI air parcels experience strong diabatic warming by turbulent fluxes and shallow convection (by +0.2 to +0.5 K h^{-1}) in the lower part of the boundary layer. A net heating rate dipole is therefore experienced by EDI trajectories upon penetration into the boundary layer, with much larger prior cooling in regions with large cloud fractions (-1 K h^{-1}, Fig. 3) than in regions with more scattered boundary layer clouds (-0.25 K h^{-1}, Fig. 3). The rapid diabatic warming in the boundary layer leads to a strong modification of the vertical structure of the cold front

and to an erosion of the cold and dry anomaly in the lower free troposphere behind the southward propagating cold front.
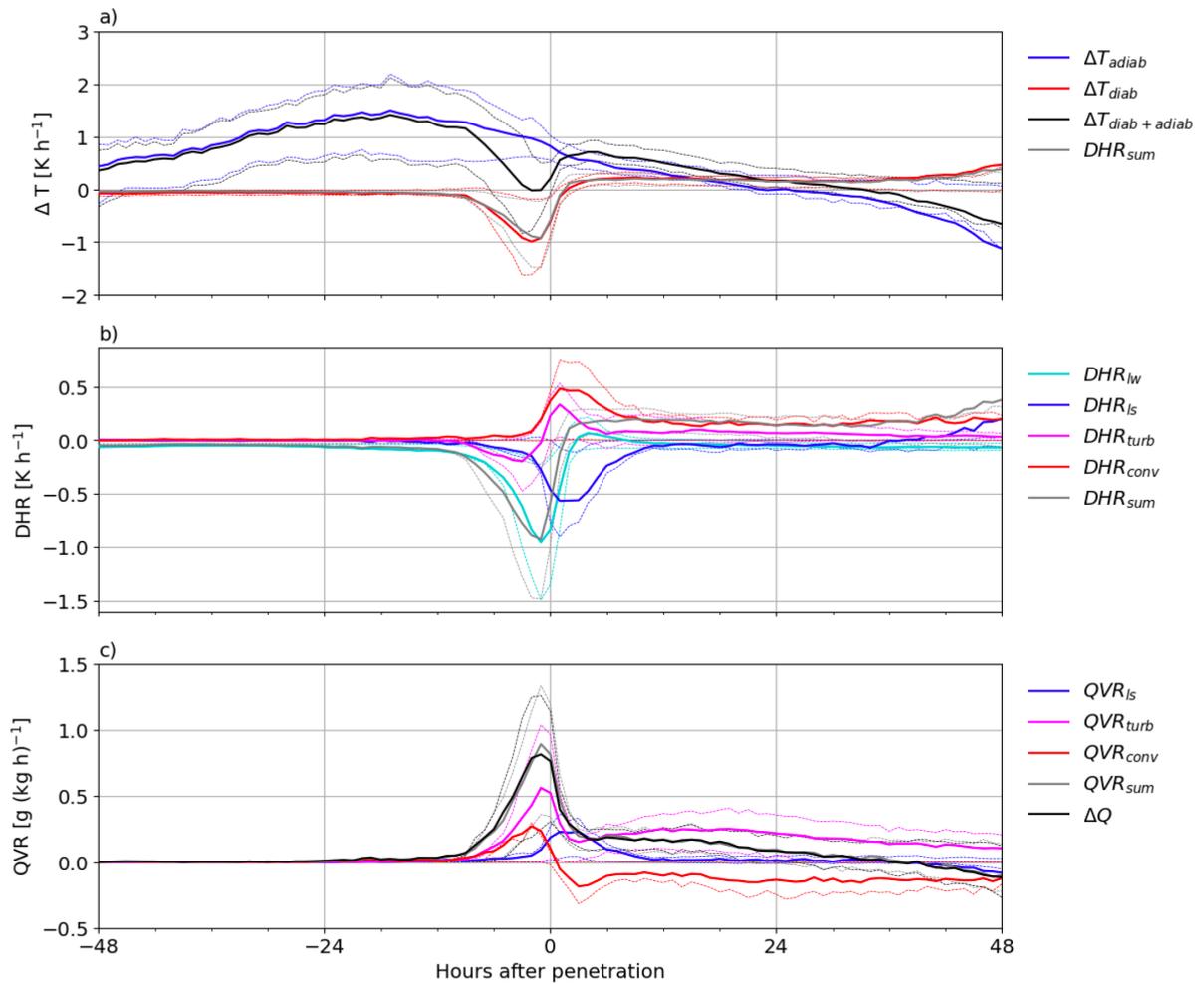

Fig. 2: Heat and water vapour budgets along the DI trajectories relative to their entry time into the boundary layer at tBLH in the time interval [tBLH -48 h, tBLH+48 h] for trajectories started at 00 UTC on 29 January in trade wind box (see Fig. 1). (a) Mean (thick lines) and 25th, 75th percentiles (thin lines) of the adiabatic (blue) and diabatic (red, grey) contributions to temperature changes along the trajectories as diagnosed from the thermodynamic energy equation applied to changes in T and q along the trajectories (red), sum of DHR from different processes (grey). (b) DHR from different processes parametrised in the model. The DHR from longwave radiation in cyan, from the large-scale microphysics in blue, from turbulence in pink, from convection in red, and the sum as in (a) in grey. The heating from shortwave radiation is small compared to the other processes and therefore not shown. (c) QVR from different processes in the model (same colors as in (b)).

The moistening of the EDI is primarily due to turbulent mixing (0.5 g kg h^{-1}) and convection (0.3 g kg h^{-1}) at cloud tops, while shortly after penetration into the boundary layer the EDI gets moistened about at equal rates by the large-scale microphysics scheme (cloud and precipitation evaporation) and turbulent mixing (0.25 g kg h^{-1}). Within the boundary layer convection acts as a drying mechanism of EDI air parcels due to condensation in clouds and to convective mixing with the free troposphere (0.15 g kg h^{-1}).

In summary, this detailed EDI case study illustrates how the rapidly subsiding EDI airstream interacts with the parametrised subgrid-scale processes at cloud top in the model, thereby affecting the thermodynamic conditions in the boundary layer and impacting the southward propagation of the cold front.
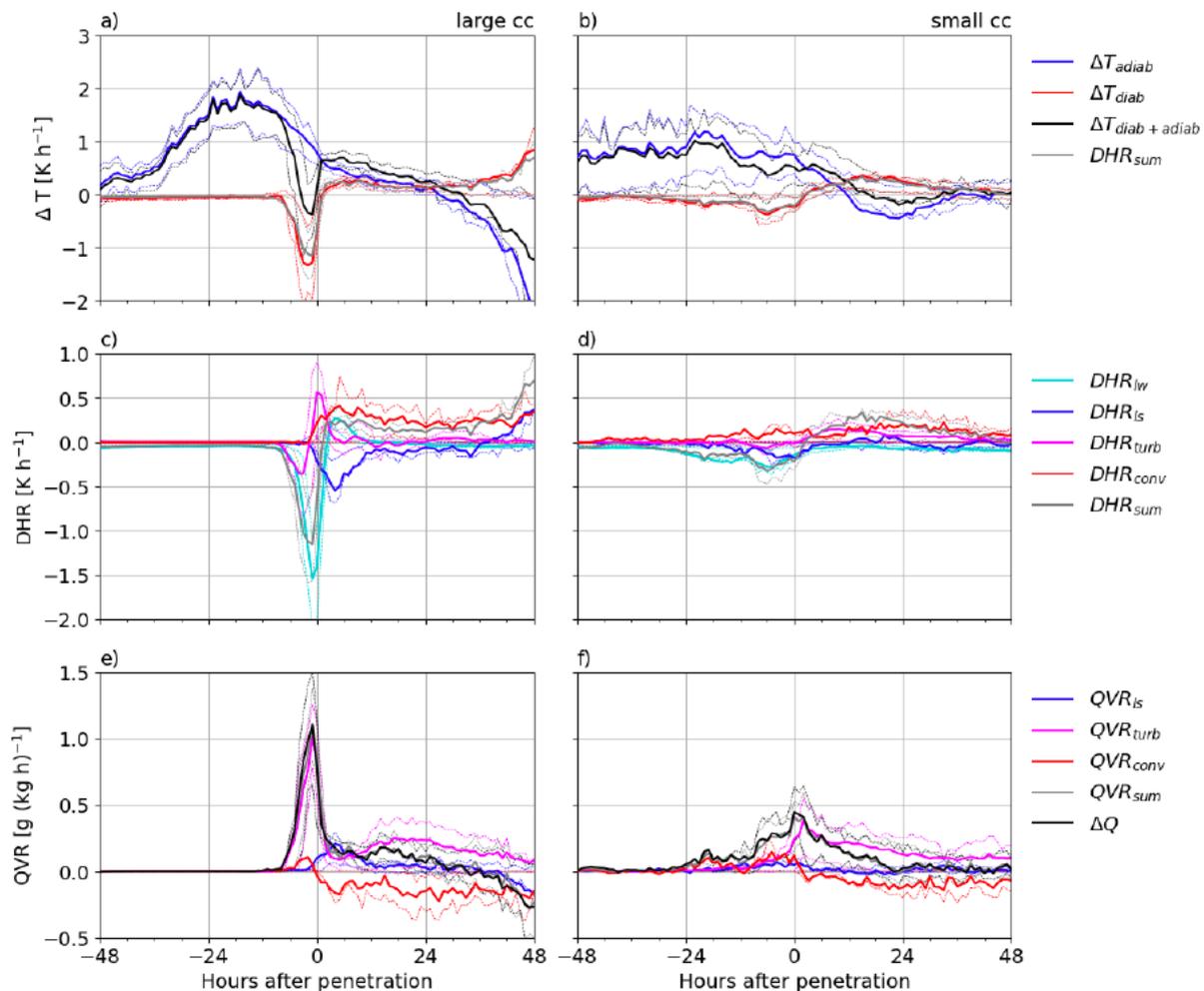
Fig. 3: As in Fig. 2 but heat and water vapour budgets for 50 DIs with largest cloud fraction (a,c,e) and 50 DIs with smallest cloud fraction (b,d,f) upon penetration into the boundary layer.

References:

Mueller, S., Diabatic processes associated with an extratropical dry intrusion reaching into the western North Atlantic trade wind region, ETH Zuerich, 2021, supervised by F. Aemisegger, M. Boettcher and L. Villiger, ETH Zuerich, Msc Thesis, 2021.

Aemisegger, F., Vogel, R., Graf, P., Dahinden, F., Villiger, L., Jansen, F., Bony, S., Stevens, B., and Wernli, H.: How Rossby wave breaking modulates the water cycle in the North Atlantic trade wind region, Weather Clim. Dynam., 2, 281–309, https://doi.org/10.5194/wcd-2-281-2021, 2021.

2) Diabatic processes in Mediterranean cyclones (A. Scherrmann, Dr. E. Flaounas)

In the PhD project of A. Scherrmann, we are investigating and quantifying the PV modification by different diabatic processes in Mediterranean cyclones which are identified in the one year simulation with the special IFS version. This simulation has been performed in the framework of the previous special project "Diabatic effects in mid-latitude weather systems". We combine the available PV tendencies with 48 hours backward trajectories (calculated using LAGRANTO) to (i) determine the most dominant diabatic process in the Mediterranean shaping the lower-tropospheric PV anomaly found in Mediterranean cyclones, and (ii) determine where with respect to the cyclone centre the PV modification occurs, to define so called "cyclonic" and "environmental" PV with which we distinguish self- and remotely-driven cyclones and the dominant process inside and

outside the cyclones. We find the cyclonic PV modification to account for the majority of the total PV changes. Particularly inside the cyclone we find convection and microphysics to produce the largest PV quantities, whereas in the environment convection and turbulence result in the largest PV changes (see. Fig. 1).
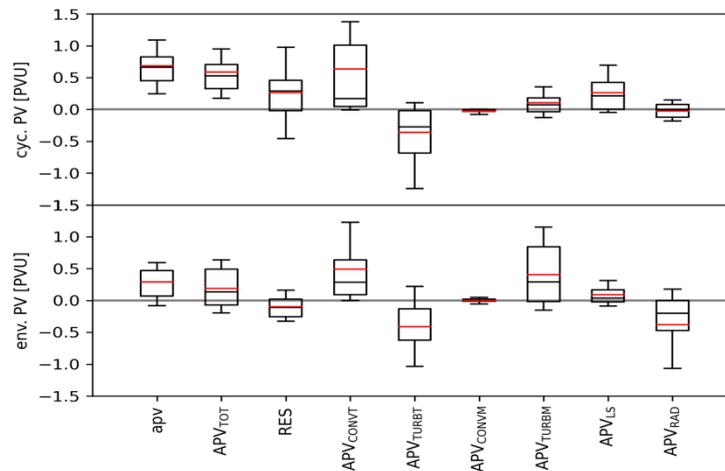

Fig. 1: Distribution of PV production in the lower-tropospheric PV anomaly in Mediterranean cyclones. (a) shows the changes produced inside the cyclone and (b) the modifications in the environment.

Furthermore, we identify regions in which different diabatic processes frequently produce large PV changes, i.e., > 0.15 PVU/h (see. Fig. 2). Large PV modification due to latent heat release by convection and microphysics (Fig. 2a, b) predominantly occurs in the Tyrrhenian, Adriatic, Ionian, and Aegean Seas, close to Cyprus, and in the Black Sea, which are mainly positive changes. Additionally, microphysics frequently results in large PV production over the European continent (Fig. 2b). Turbulence results in large PV changes near the mountains, over Tunisia and Egypt, and along coastlines (Fig. 2c, d). For turbulent processes, the regions of frequent PV production and destruction tend to overlap, indicating that whether PV is produced or destroyed highly depends on the current local conditions.
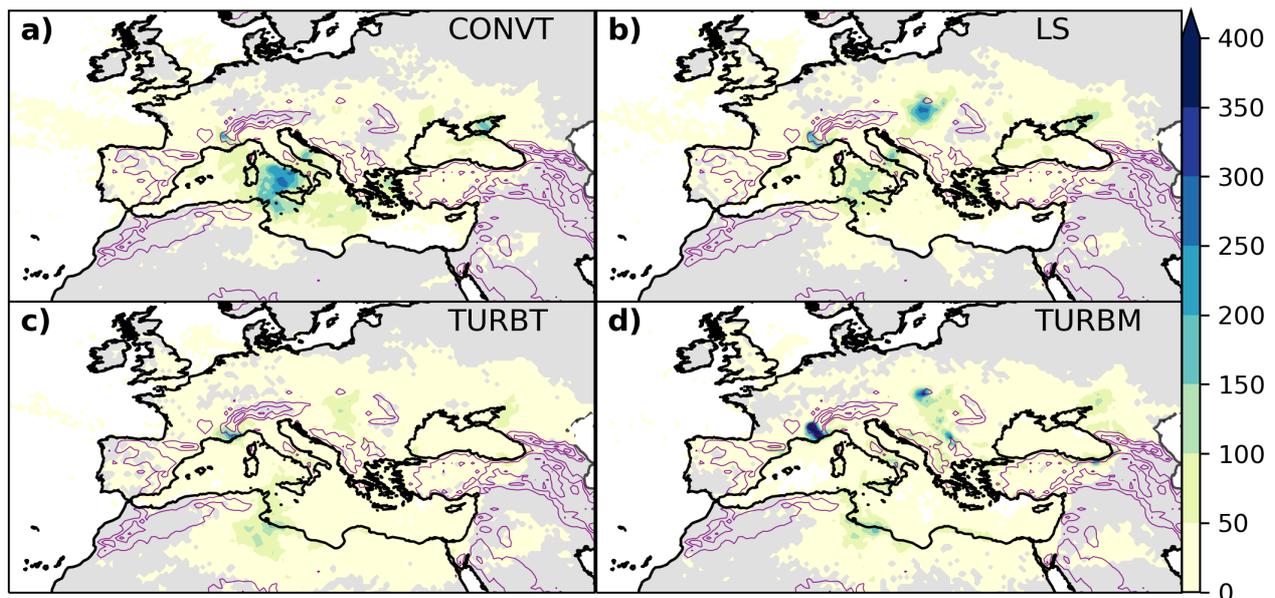

Fig. 2: Frequency maps of large PV modifications > 0.15 PVU/h due to (a) convective temperature tendencies; (b) microphysics; (c) turbulent temperature tendencies; (d) turbulent momentum tendencies.

3) Moisture cycle in an extratropical cyclone (Simon Eschle, Dr. Maxi Böttcher, Dr. Hanin Binder, Dr. Hanna Joos)

In a Master thesis (Eschle, 2022), the moisture sources and cycles of an extratropical cyclone have been investigated with data from an IFS simulation with hourly output of moisture tendencies from subgrid-scale processes (turbulence, convection and cloud microphysics) and from advection. The extratropical cyclone occurred in the North Pacific in April 2017. The goals of the thesis were to (1) determine the processes that were responsible for the moisture uptake in the cyclone, (2) identify the processes that moistened the airstreams around the cold front, (3) assess whether moisture recycling, i.e. the reuptake of moisture, occurred and (4) examine which role below-cloud processes (rain evaporation and sublimation of snow and ice) played. Lagrangian trajectories have been used to examine the pathways of air and moisture for a cross section through the cold front at the time of the strongest intensity of the cyclone.

It was found that advection, i.e. the transport of moisture, was the most important process leading to moisture changes (both moisture uptake and moisture loss) in different parts of the cyclone at the time of its strongest intensity. Turbulent processes were crucial for the uptake of moisture over the cold sector, whereas convection and large-scale cloud processes were mainly associated with moisture loss at the cold and warm fronts. The individual microphysical processes from the large-scale cloud scheme revealed that the moisture loss was mainly associated with condensation, followed by deposition of ice (Fig. 1a,b). At the same time, moisture uptake due to snow and ice sublimation and to a lesser extent due to cloud evaporation also played an important role at the cold and warm fronts (Fig. 1c-e). One dry intrusion airstream experienced moisture uptake through turbulent processes when approaching the cold front. Two branches of the warm conveyor belt (WCB) were moistened by snow and ice sublimation at the cold front at the time of the strongest intensity of the cyclone. During the subsequent ascent, they experienced condensation and, later on, deposition of ice and snow. Air that was simultaneously moistened by rain evaporation and turbulence behind the surface cold front in the first place exhibited a WCB-like ascent afterwards. During its ascent, this air also encountered condensation. All these WCB and WCB-like airstreams partly revealed moisture recycling. During their ascents, liquid and ice clouds were formed by moisture originating from snow and ice sublimation or rain evaporation within the same cyclone. The results of this Master thesis highlight (i) the dominant contribution of advection to the moisture budget, (ii) the prominent role of snow and ice sublimation to the moisture budget and cycle, and (iii) that in this particular cyclone moisture recycling was observed.
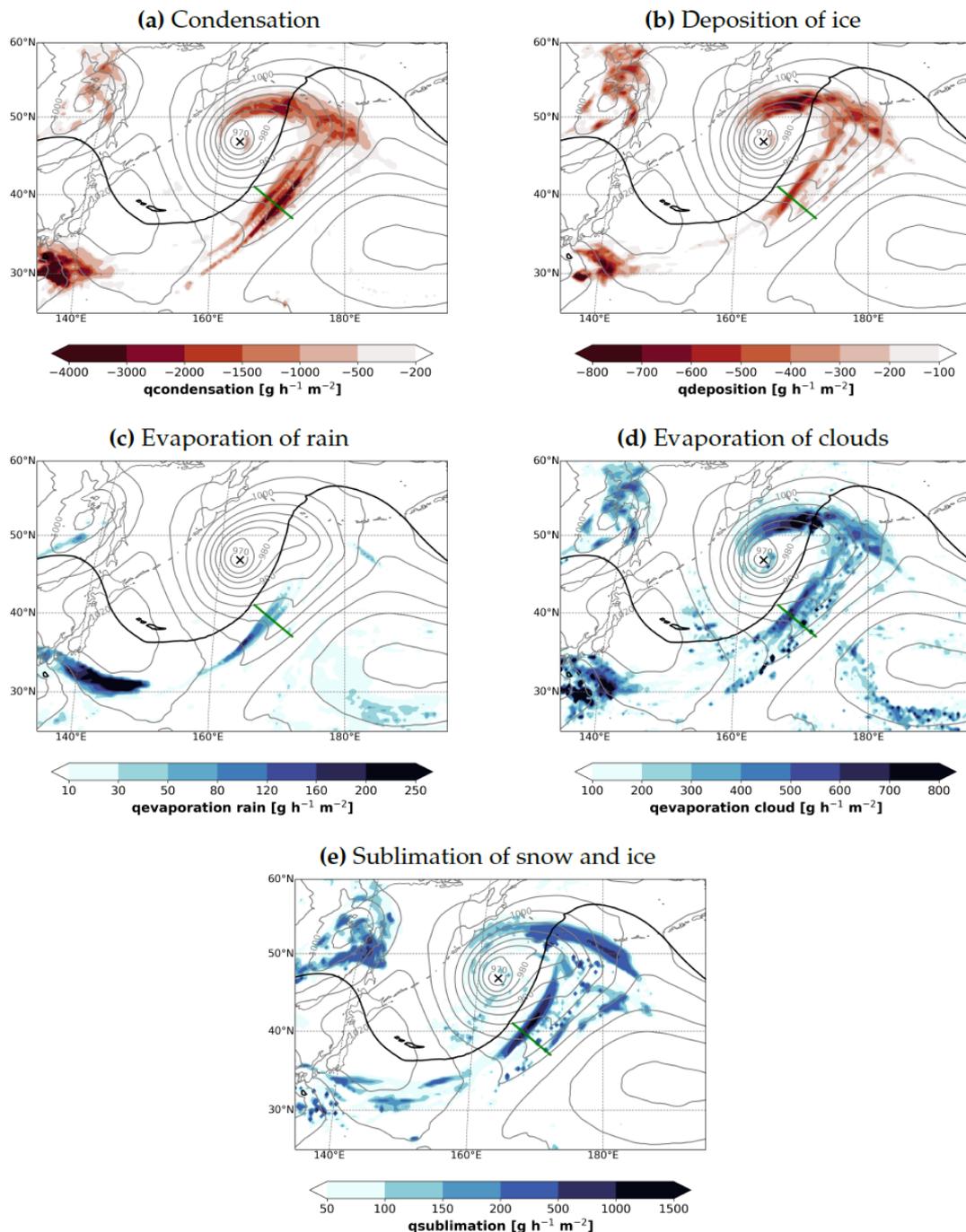
Fig. 1: Vertically integrated moisture tendencies (g h^{-1} m^{-2}; shading) of the individual microphysical processes from the large-scale cloud scheme at the time of the strongest intensity of the extratropical cyclone, at 17 UTC 10 April 2017. Shown are (a) condensation, (b) deposition of ice, (c) evaporation of rain, (d) evaporation of clouds, and (e) sublimation of snow and ice. Blue colors indicate regions with moisture uptake and red colors regions with moisture loss. Note that different color scales are used for each tendency. In addition, the grey contours show sea level pressure (every 5 hPa) and the thick black line the 2 pvu contour at 320 K. The black cross marks the position of the cycle center.

Reference:

Eschle, S., Moisture cycle in an extratropical cyclone, MSc thesis ETH Zuerich, 2022, supervised by M. Böttcher, H.Binder and H. Joos

4) Modification of potential vorticity by radiation in the extra-tropics (Noè Zardi, Dr. Roman Attinger, Dr. Sophia Schäfer (German Weather Service), Dr. Hanna Joos)

The 1-year simulation with the IFS special version which allows for hourly output of all tendencies due to parameterized physics is used in order to investigate in which synoptic situations in the extratropics, radiative heating rates are able to modify potential vorticity in a way that the formed PV anomalies have the potential to modify the atmospheric circulation. Therefore, in the 1-year dataset all gridpoints, where radiative PV rates accumulated over 24 hours contribute substantially to the total observed PV anomaly, have been identified. Based on this analysis, two case studies have been selected where (i) radiative PV rates contribute to a positive low-level PV anomaly in the North Pacific that develops into a low pressure system and (ii) radiation leads to the development of a pronounced negative PV anomaly in the upper troposphere.

As an example, in Figure 1, diabatic PV rates that have been accumulated along 24h backward trajectories are shown on the 310 K isentrope, separately for contributions from shortwave heating (SW APV), longwave heating (LWH APV), longwave cooling (LWC APV) as well as the total diabatic PV rates (Tot APV). The black line shows the position of the tropopause (here shown as the 2 pvu isoline) and the blue line encloses a region with PV < 0 pvu.
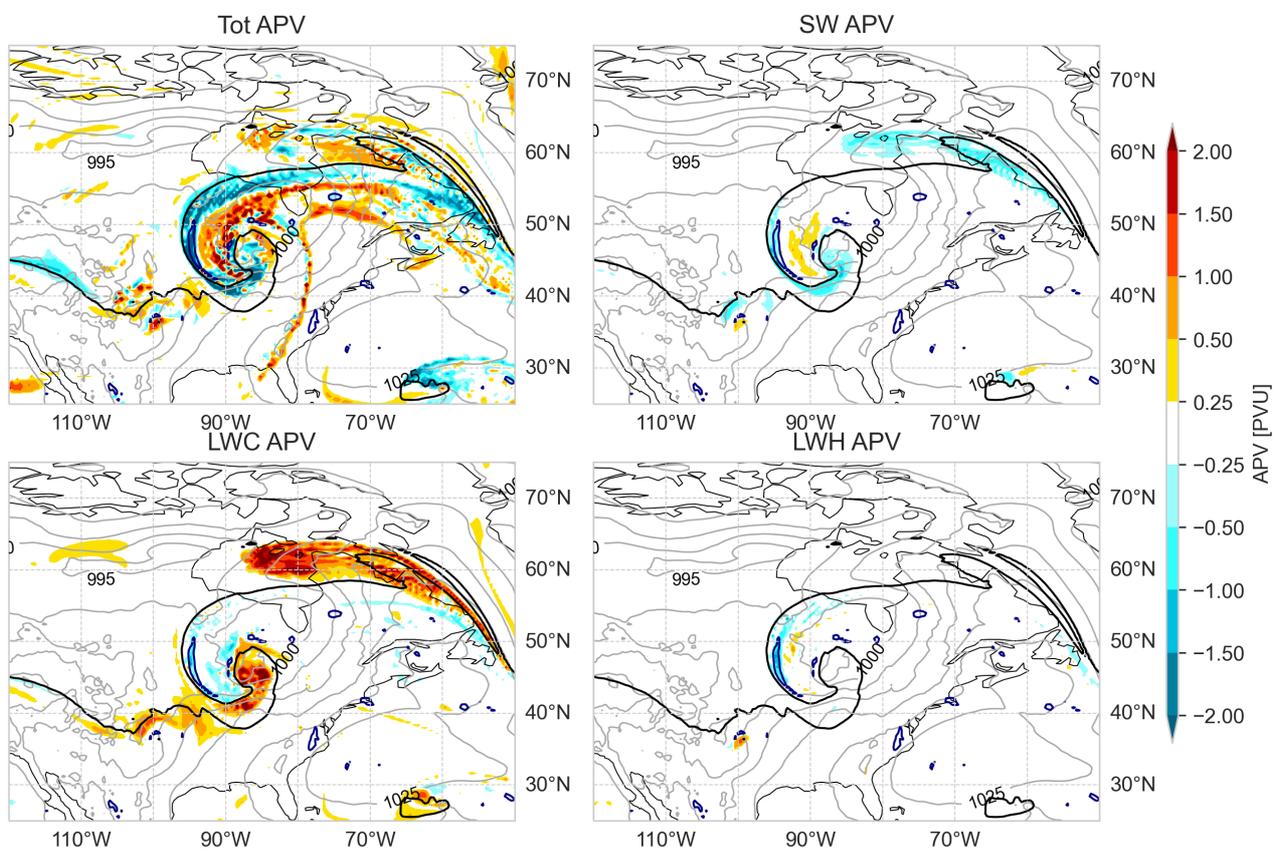

Fig. 1: 24 h accumulated diabatic PV rates (colours) on the 310 K isentrope. Tot APV denotes the total PV modification due all diabatic processes, SW APV due to shortwave heating, LWC APV due to longwave cooling and LWH APV due to longwave heating. The black line shows the position of the tropopause (2 pvu isoline) on the 310 K isentrope, and the blue line the 0 pvu isoline.

It can be seen that in the region with PV < 0 pvu, all three radiative heating rates contribute to the destruction of PV in the last 24h before their arrival in this region. This is possible due to a favorable way of the airmasses relative to the heating/cooling rates induced by radiation. This and other case studies where radiation directly modifies PV will be analyzed in order to increase our understanding of the interaction of radiation and dynamics in the extratropics.

5) Diabatic heating and PV rates in a warm conveyor belt in the ICON and IFS model (Dr. Annika Oertel)

For the inter-model comparison of heating and PV rates from individual microphysical processes in WCBs in the IFS and ICON models, 4-day global free-running simulations of a WCB case study in October 2016 in the North Atlantic (Fig. 1) were conducted with the IFS and ICON models, respectively. The IFS is run at approx. 9 km horizontal grid spacing (TCo1279) and the ICON is run at a resolution of approx. 13 km (R3B07). Both simulations are initialized from the IFS analysis and remapped to a regular 0.2° x 0.2° grid. Trajectories are started in the North Atlantic region from an equidistant grid at seven vertical pressure and respective height levels in the lower troposphere. While the simulations are quasi-identical at initialization, the larger-scale flow diverges substantially after 96 hours lead time. The comparison of WCB trajectories, defined as trajectories that ascend at least 600 hPa within 48 h, shows that in the IFS model the WCB trajectories do not only ascend faster on average (Fig. 2a), but also a substantially larger number of WCB trajectories is found in the IFS simulation. In total, more than twice as many WCB trajectories ascending in the entire North Atlantic region during the 4-day simulation are identified in the IFS model compared to the ICON model. Interestingly, WCB trajectories in the IFS on average descend before their fastest 600 hPa ascent, which is not represented in the ICON model, where trajectories remain below 900 hPa prior to their ascent. The diabatic heating during the ascent is comparable in both simulations and on average amounts to 23 K in ICON and 26 K in the IFS (Fig. 2c). WCB trajectories in the IFS reach a higher isentropic surface, due to their slightly higher diabatic heating and as they start their ascent at a higher isentropic surface.

Preliminary results show that the total hydrometeor content along the WCB ascent is larger in the IFS model, in particular during the rapid initial ascent phase (Fig. 2d). The separation into the individual hydrometeor types shows distinct differences in the detailed representation of the cloud structure, and between the separation in liquid and frozen hydrometeors. In the IFS simulation rain and snow water content are the dominant hydrometeor types, and both reach higher values than in the ICON model, where cloud water content reaches the highest values. Ice water content has similar values in both models and becomes most important in the WCB outflow region in the upper troposphere. Ongoing analysis will compare detailed diabatic heating and potential vorticity rates along WCB ascent, and the influence of the different microphysical parameterizations on the cloud structure, heating patterns, and potential vorticity distribution.
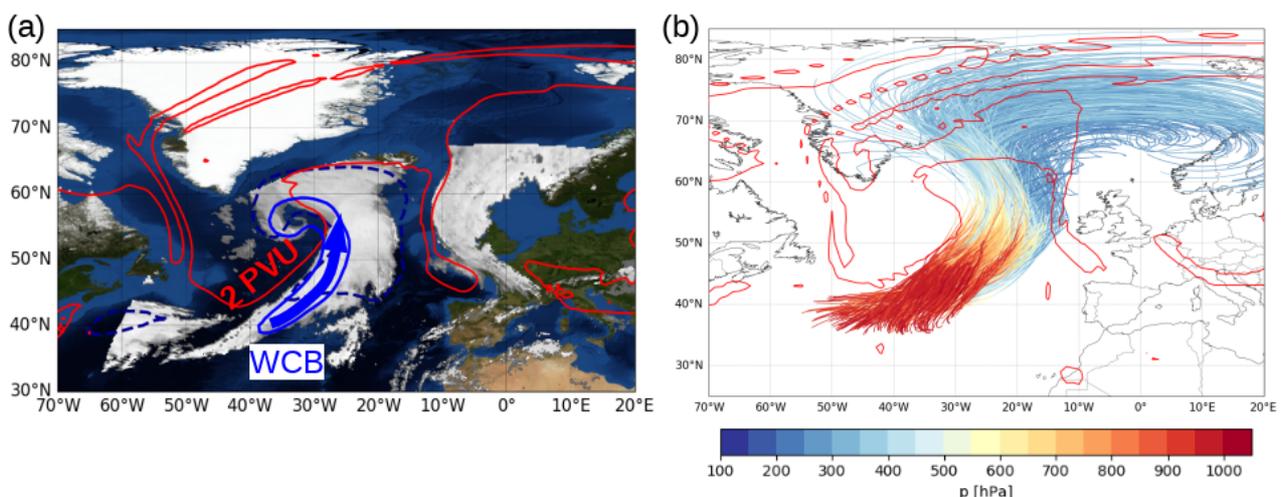

Fig. 1: (a) Satellite cloud top pressure (MSG-3 SEVIRI) of the WCB cloud band in October 2016 and (b) WCB trajectories calculated from 3D ICON output coloured according the pressure. The red line shows 2 PVU at 320 K from (a) ERA-5 reanalysis and (b) the ICON simulation.
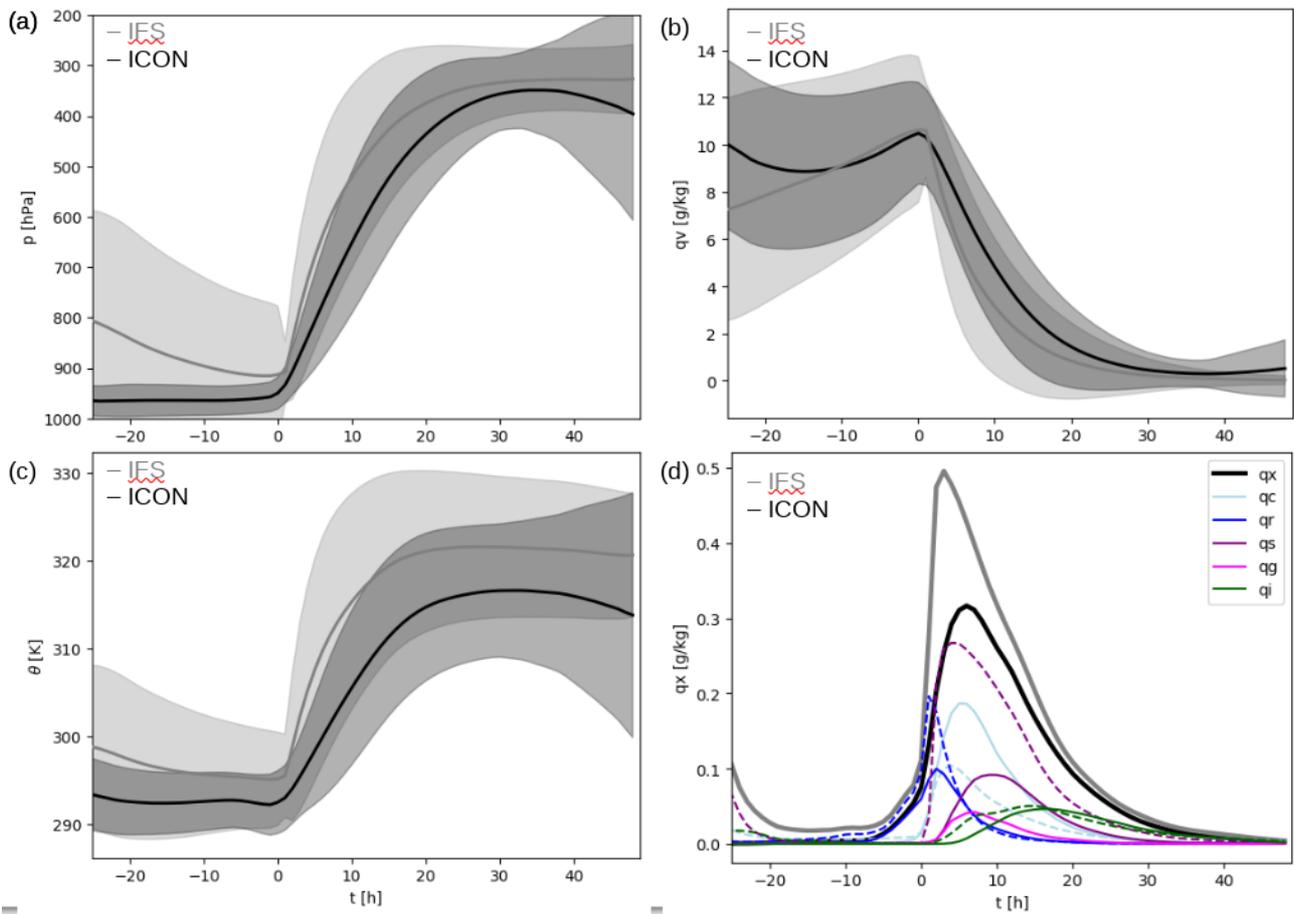
Fig. 2: Mean evolution plus standard deviation (shading) of (a) pressure (in hPa), (b) specific humidity (in g/kg), (c) potential temperature (in K), and (d) total hydrometeor content (g/kg) along WCB trajectories in the IFS (grey) and ICON (black) simulations. (d) additionally shows rain water content (qr, blue), cloud water content (qc, light blue), ice water content (qi, green), and snow water content (qs, purple) for the IFS (dashed) and ICON (solid) simulations. Graupel water content (qg, magenta) from the ICON simulation is also shown.